THE JOURNAL OF PHYSICAL CHEMISTRY Letters

Letter

pubs.acs.org/JPCL

Bias-Switchable Permselectivity and Redox Catalytic Activity of a Ferrocene-Functionalized, Thin-Film Metal–Organic Framework Compound

Idan Hod,[†] Wojciech Bury,[†,‡] Daniel M. Gardner,[†] Pravas Deria,[†] Vladimir Roznyatovskiy,[†] Michael R. Wasielewski,[†] Omar K. Farha,*[,†,§] and Joseph T. Hupp*[,†]

[†]Department of Chemistry, Northwestern University, 2145 Sheridan Road, Evanston, Illinois 60208, United States

[‡]Department of Chemistry, Warsaw University of Technology, Noakowskiego 3, 00-664 Warsaw, Poland

[§]Department of Chemistry, Faculty of Science, King Abdulaziz University, Jeddah, Saudi Arabia

Supporting Information

ABSTRACT: The installation of ferrocene molecules within the wide-channel metal–organic framework (MOF) compound, NU-1000, and subsequent configuration of the modified MOF as thin-film coatings on electrodes renders the MOF electroactive in the vicinity of the ferrocenium/ferrocene (Fc^+/Fc) redox potential due to redox hopping between anchored $Fc^{+/0}$ species. The observation of effective site-to-site redox hopping points to the potential usefulness of the installed species as a redox shuttle in photoelectrochemical or electrocatalytic systems. At low supporting electrolyte concentration, we observe bias-tunable ionic permselectivity; films are blocking toward solution cations when the MOF is in the ferrocenium form but permeable when in the ferrocene form. Additionally, with ferrocene-functionalized films, we observe that the MOF's pyrene-based linkers, which are otherwise reversibly electroactive, are now redox-silent. Linker electroactivity is fully recovered, however, when the electrolyte concentration is increased 10-fold, that is, to a concentration similar to or exceeding that of an anchored shuttle molecule. The findings have clear implications for the design and use of MOF-based sensors, electrocatalysts, and photoelectrochemical devices.

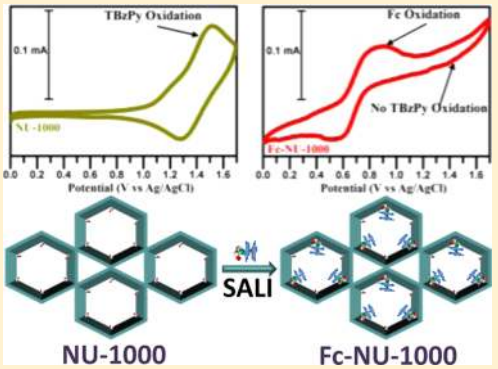

The development of increasingly general methods for assembling surface-supported metal–organic frameworks (SURMOFs)[1−9] in thin-film form promises to open up new science and new possibilities for their application. Example applications could include electrochemical catalysis,[10] integration with silicon[11,12] for electronic sensing of volatile chemicals, and membrane-based separation of chemical species.[13] Much of our own interest in porous, crystalline thin-film MOFs centers on their potential as light-harvesting arrays relevant to solar energy conversion.[14−17] The most sophisticated SURMOF synthesis methods are automated and offer layer-by-layer control (i.e., molecular-scale control) over thin-film composition and component molecule orientation. Given these capabilities, one could envision building panchromatic antenna systems containing a half of a dozen or more spectrally overlapping chromophores positioned to facilitate long-range energy transfer—systems that could constitute functional analogues of the natural photosynthetic light-harvesting apparatus.[18] Toward this goal, we have been able to synthesize and functionally characterize MOFs displaying (a) long-range directional energy transfer (EnT) within isolated porous crystals,[19] (b) linker-to-heterolinker and linker-to-terminus-molecule EnT within isolated crystals[20] and surface-immobilized films,[21] respectively, and (c) sensitization of isolated MOF crystals with quantum dots.[22]

For many solar energy conversion schemes, an additional requirement is that the MOF film be redox-reactive, thereby facilitating charge transport (via hopping) through the framework and into a redox-driven chemical catalyst, current collector (an electrode), or both. Hopping could occur between neighboring MOF linkers/chromophores or, by analogy to solid-state dye-sensitized solar cells, could be delegated to redox shuttle molecules. A handful of reports have appeared on linker-to-linker redox hopping in MOFs,[10,23−25] but none are based on framework-tethered shuttle molecules. Here, we report that ferrocene can be controllably installed within the broad (ca. 30 Å) diameter channels of the platform MOF, NU-1000 (see Scheme 1), and that redox reactivity for the full complement of installed shuttle molecules can be readily observed via voltammetry when the modified MOF is configured as an electrode-supported film. Consistent with previous observations with a closely related material, NU-901,[24] we also observe electrode-supported, thin-film redox reactivity

Received: January 5, 2015
Accepted: January 26, 2015
Published: January 26, 2015

DOI: 10.1021/acs.jpclett.5b00019
J. Phys. Chem. Lett. 2015, 6, 586−591

Scheme 1. (A) NU-1000's Chemical Structure, (B) NU-1000's Hexagonal and Trigonal 1D Channels, (C) Illustration of Ferrocene Functionalization Using SALI[a]

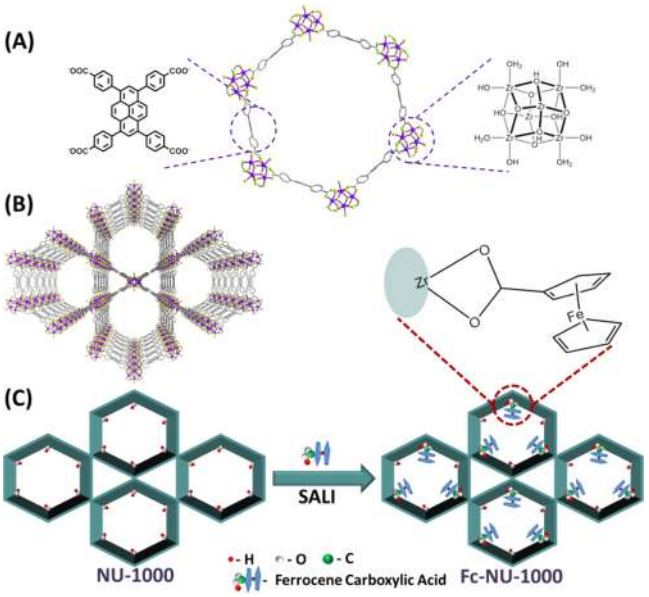

[a]We assume that SALI occurs only in the large hexagonal channels and not the sterically more demanding trigonal channels.

based on reversible oxidation of the full complement of pyrene-containing linkers of NU-1000. To our surprise, however, linker-based redox reactivity is undetectable in the redox-shuttle modified version of the MOF. As described below, this unexpected behavior is attributable to bias-switchable anionic permselectivity (cation exclusion (Donnan exclusion)) within the MOF itself. The permselectivity is engendered by installation and subsequent electrochemical oxidation of the tethered redox shuttle, thereby creating a mesoporous MOF matrix featuring fixed cationic sites. The permselectivity can be switched off by appropriately altering the applied electrochemical potential or by substantially boosting the concentration of the supporting electrolyte.[26−30] These observations have important implications for the design and use of porous MOFs as building blocks for catalytic electrodes, photoelectrodes, and overall photochemical energy conversion systems.

Due to its excellent chemical stability, including stability in neutral, acidic, and basic aqueous solutions, and due to the comparative ease with which its channels can be chemically tailored, the Zr-based MOF,[16,31−36] NU-1000,[37] was chosen for redox functionalization. The previously described solvent-assisted ligand incorporation (SALI)[38,39] method (Scheme 1) was used to attach a singly carboxylated version of the well-known redox molecule, ferrocene (Fc), to the $Zr_6(\mu_3\text{-}O)_4(\mu_3\text{-}OH)_4(OH)_4(OH_2)_4$ nodes[40] of microcrystalline powder samples of NU-1000. ^{1}H NMR analysis of ferrocene-modified samples following digestion revealed a loading of one ferrocene molecule per node (Figure S1, Supporting Information). For electrochemical investigation, thin films of both the ferrocene-free and ferrocene-derivatized MOF (termed NU-1000 and Fc-NU-1000, respectively) were formed on conductive glass electrodes (fluorine-doped tin oxide (FTO)) from toluene suspensions of the MOF via electrophoretic deposition, as recently described[4] (see also related work by Hwang et. al[41]) and as further detailed in the Supporting Information.

Figure 1 shows the electrochemical (cyclic voltammetry (CV)) responses of electrode-attached films of NU-1000 and

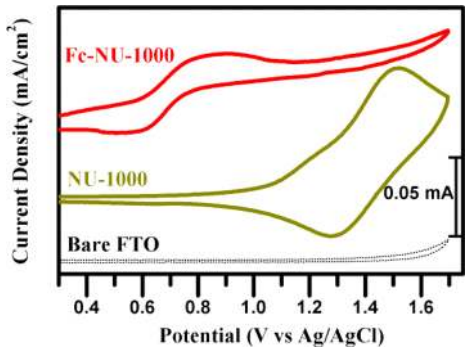

Figure 1. CVs of films of NU-1000 and Fc-NU-1000 immersed in a solution of 0.05 M $TBAPF_6$ in acetonitrile as the solvent. NU-1000 clearly shows a reversible electro-oxidation of the TBzPy linker. However, Fc-NU-1000 exhibits only a chemically reversible oxidation wave for anchored ferrocene. The black dashed line shows a scan of a bare FTO electrode in the same conditions (the electrode's active surface area is 1 cm^2, and the scan rate is 50 mV/s).

Fc-NU-1000 in 0.05 M $TBAPF_6$ (TBA^+ = tetrabutylammonium) in acetonitrile as the solvent. As illustrated by a voltammetry wave with anodic and cathodic peaks at ∼1.5 and 1.3 V Ag/AgCl, NU-1000 (green curve) exhibits behavior consistent with chemically reversible electro-oxidation of coordinated 1,3,6,8-tetrakis(*p*-benzoate)pyrene to its radical cation form ($TBzPy^+$).[24] Visible-region spectroelectrochemical measurements, discussed further below, corroborate the interpretation.

Fc-NU-1000 behaves in a strikingly different manner; again, see Figure 1. A reversible oxidation peak, assignable to incorporated ferrocene, is observed at around 0.8 V. Extension of the CV potential range to +1.7 V, however, yields no trace of TBzPy-centered redox reactivity. Continuous-wave electron paramagnetic resonance (CW-EPR) measurements (taken at 85 K) of various films removed by scraping corroborate the behavioral difference. Briefly, four kinds of films were examined: Fc-NU-1000, Fc-NU-1000 that had been held at 1.6 V versus Ag/AgCl in a 0.05 M $TBAPF_6$ acetontrile solution (Fc-NU-1000-ox), NU-1000, and NU-1000 that had been held at 1.6 V in a 0.05 M $TBAPF_6$ acetontrile solution (NU-1000-ox), that is, positive of the formal potential for TBzPy oxidation. As shown in in Figure 2, the first three yield no CW-EPR signal at a position corresponding to oxidized pyrene, whereas a scraped film of NU-1000-ox produces a sizable signal. Notably, the signal line shape and position agree well with the previously reported CW-EPR spectrum of electro-oxidized films of the pyrene-containing MOF NU-901,[24] as well as those of other pyrene-based radical cations.[42,43] (As can be seen in Figure S2 (Supporting Information), expending the CW-EPR magnetic field window reveals a broad signal for Fc-NU-1000 ox, which corresponds to a signal for ferrocenium species.) Finally, visible-region spectroelectrochemical measurements for electrode-supported films of NU-1000 and Fc-NU-1000 confirm that TBzPy is present in both, but only in NU-1000 is it electrochemically oxidizable (Figure S3, Supporting Information).

DOI: 10.1021/acs.jpclett.5b00019
J. Phys. Chem. Lett. 2015, 6, 586−591

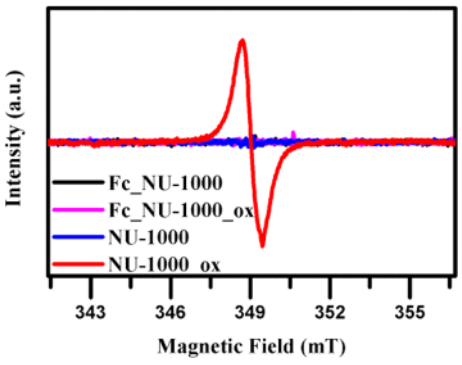

Figure 2. Results from CW-EPR measurements of samples of Fc-NU-1000 and NU-1000, without and with ("ox") prior potentiostatting at +1.6 V. Only the sample designated "NU-1000-ox" (see text) yielded an EPR signal in the region expected for a pyrene radical.

The small size of an anchored ferrocene molecule (~5 Å diameter) relative to the channel diameter of NU-1000 (31 Å) permits us to rule out physical blocking of charge-compensating ions as an explanation for the unexpected shutdown of linker electrochemistry in electrode-immobilized Fc-NU-1000. A more attractive explanation is that installation and oxidation of anchored shuttle molecules (to ferrocenium, Fc^+) converts the MOF to a form that, while remaining permeable to solvent molecules and electrolyte anions, is now electrostatically blocking toward free cations. In other words, the MOF, in Fc^+ form, is permselective for anions. Thus, at low ionic strength, charge balance within the MOF would be achieved by recruiting from the in-filling and surrounding solution one PF_6^- per ferrocenium ion generated. Additionally, the high local concentration of fixed-site cations (i.e., anchored Fc^+) should result in expulsion of most TBA^+ (a Donnan exclusion effect[44]) and, therefore, most excess PF_6^-. To maintain charge balance within the MOF, subsequent electro-oxidation of the neutral linker to its cationic form would require either expulsion of an equivalent amount of TBA^+ (unavailable at low ionic strength and therefore impossible to expel) or recruitment of additional electrolyte anions from the in-filling solution (again unavailable due to exclusion of salt by the cationic framework material).

Scheme 2 illustrates the proposed explanation. If the scheme is correct, the putative film permselectivity should disappear, the Fc^+-containing MOF should become permeable to the overall electrolyte, and linker electroactivity should be restored, once the electrolyte concentration is made similar to, or greater than, the concentration of fixed-site cations (ferrocenium ions) within the MOF channels. A loading of one ferrocene/ferrocenium per node corresponds to an in-channel concentration of about 0.3 M. Figure 3 shows the cyclic voltammetric behavior of Fc-NU-1000 at low and high electrolyte concentrations. Notably, linker electroactivity is restored when the electrolyte concentration is 0.5 M.

Scheme 2. Schematic Illustration of the Processes Occurring during Reversible Electrochemical Induction of Anionic Permselectivity in Fc-NU-1000

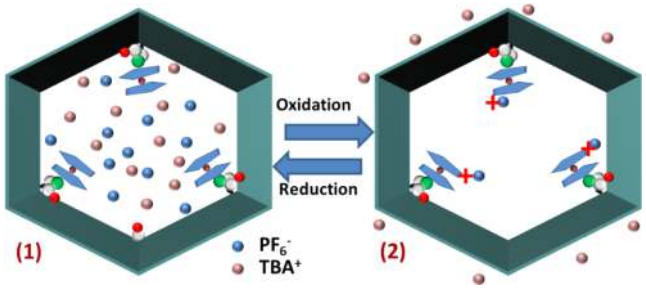

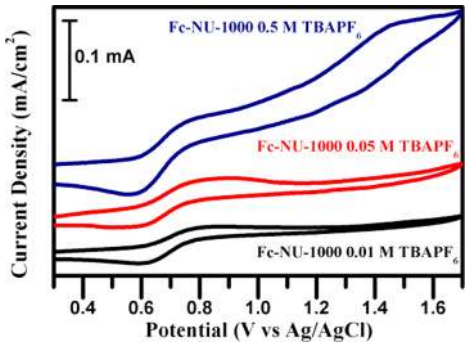

Figure 3. CVs comparing between Fc-NU-1000 at different $TBAPF_6$ supporting electrolyte concentrations. At low electrolyte concentrations, TBzPy linker oxidation is shut down. However, at an electrolyte concentration larger than that of the fixed Fc^+ sites, linker electroactivity is restored. (The electrode's active surface area is 1 cm^2, and the scan rate is 50 mV/s.)

A corollary to the above is that for positively charged *solution-phase* species having formal potentials positive of the shuttle's potential, the electrode-immobilized film should be blocking (at low ionic strength) toward their oxidation. These species would encounter a cation-excluding, permselective MOF. For similar species having formal potentials negative of that of the shuttle, however, the electrode-immobilized film should not be blocking toward their oxidation. Thus, these species would encounter a neutral MOF that is permeable to both anions and cations. Additionally, the anchored shuttle molecules should be capable, at more positive potentials, of mediating the oxidation of solution-phase species, that is, redox catalytic behavior should be possible.

To test these ideas, we examined the electrochemical response of MOF films to either $Fe(bpy)_3^{2+}$ or $Co(phen)_3^{2+}$ at 2 mM (bpy = 2,2′-bipyridine; phen = 1,10-phenanthroline) in low ionic strength solutions. Results for the iron complex are shown in Figure 4. Voltammetry recorded at a bare FTO electrode shows a reversible wave just beyond 1 V for oxidation of $Fe(bpy)_3^{2+}$ to $Fe(bpy)_3^{3+}$. Similar behavior is observed at an electrode covered with NU-1000, albeit with the addition of a wave assignable to linker oxidation at further positive potential. The absence of a return wave (reduction wave) for the linker is indicative of mediated (i.e., redox catalytic) oxidation of $Fe(bpy)_3^{2+}$ in addition to unmediated oxidation. At an electrode coated with Fc-NU-1000, in contrast, the electrochemical oxidation of $Fe(bpy)_3^{2+}$ is blocked, as expected if the MOF is behaving as a cation-excluding, permselective network containing node-anchored ferrocenium.[30,45,46]

Figure 5 shows the corresponding results with $Co(phen)_3^{2+}$. Notably, the formal potential for oxidation of this complex (~0.5 V) is significantly less positive than that of the MOF-anchored redox shuttle. At bare FTO, a chemically reversible but electrochemically sluggish wave is seen. (Slow kinetics is a consequence of a redox-induced spin change at the cobalt center and resulting large vibrational reorganization energy.[47]) For NU-1000 electrodes, a reversible redox wave for $Co(phen)_3^{2+/3+}$ is seen, albeit with even slower electrochemical

DOI: 10.1021/acs.jpclett.5b00019
J. Phys. Chem. Lett. 2015, 6, 586−591

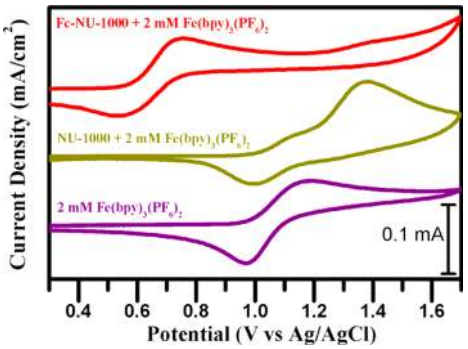

Figure 4. CVs of solutions containing 2 mM $Fe(bpy)_3^{2+}$ using working bare FTO (purple), Fc-NU-1000-coated FTO (red), or NU-1000-coated ITO (green) working electrodes. The formal potential of $Fe(bpy)_3^{3+/2+}$ is positive of that of the MOF-anchored $Fc^{+/0}$ couple. As a result, $Fe(bpy)_3^{2+}$ is excluded from the Fc-NU-1000 channels and blocked from reaching the underlying electrode; hence, its oxidation is prevented. However, when the nonpermselective NU-1000 is used, the $Fe(bpy)_3^{2+}$ oxidation wave is observed. (The electrode's active surface area is 1 cm^2, and the scan rate is 50 mV/s.)

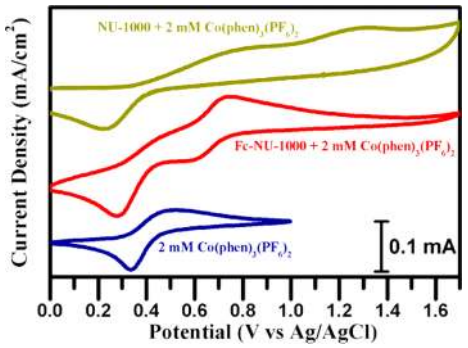

Figure 5. CVs of $Co(phen)_3^{2+}$ solutions recorded on bare FTO (blue), Fc-NU-1000-coated FTO (red), and NU-1000-coated FTO (olive) electrodes. Due to the fact that its redox potential is more cathodic than Fc/Fc^+, $Co(phen)_3^{2+}$ can enter the channels of Fc-NU-1000, and its oxidation wave is seen, similarly to the case of NU-1000. (The electrode'ss active surface area is 1 cm^2, and the scan rate is 50 mV/s.)

kinetics than that at bare FTO. In addition, TBzPy linker oxidation is observed at ~1.3 V. The fact that a return wave is absent in this case, is a result of mediated oxidation of $Co(phen)_3^{2+}$ by the TBzPy linker. For electrodes coated with Fc-NU-1000, overlapping voltammetric waves for the cobalt complex and the anchored ferrocene molecule are evident, albeit with distortions that suggest that in addition to direct oxidation, mediated (redox catalytic) oxidation of $Co(phen)_3^{2+}$ is occurring. Thus, these results indicate the permeability of Fc-NU-1000 with respect to solution-phase cations when the MOF exists in neutral form (Fc^0 form).

In summary, the broad hexagonal channels of electrophoretically deposited films of the redox-active MOF, NU-1000, can be readily functionalized with ferrocene carboxylate via solvent-assisted ligand incorporation (i.e., $R\text{-}COO^-$ displacement of nonstructural water and hydroxo ligands from the MOF's hexazirconium(IV) nodes). Under the synthesis conditions examined, the ferrocene loading reaches about one molecule per node, corresponding to a molar concentration of about 0.3. The installed molecules are electrochemically addressable, implying effective site-to-site redox hopping and potential usefulness as a redox shuttle in photoelectrochemical or electrocatalytic systems.

At low supporting electrolyte concentration (50 mM), electrochemical oxidation of the node-anchored ferrocene molecules renders the otherwise porous MOF films largely blocking toward solution cations—a Donnan-equilibrium exclusion effect. A striking consequence is the elimination of electroactivity of the otherwise reversibly oxidizable tetraphenyl-pyrene linkers of the MOF film, a finding that is corroborated by spectroelectrochemical measurements of films and CW-ESR measurements of MOF material after potentiotstatic treatment and removal from electrodes. The effective concentration of the linker in the film environment is ~0.5 M. When the electrolyte concentration is raised to match this value, linker electroactivity is restored.

A second consequence is an inability, at low supporting electrolyte concentration, to elicit significant direct oxidation of dissolved, redox-active cationic complexes, although indirect oxidation via redox catalysis, with SALI-$Fc^{+/0}$ as the redox mediator, is observable. When the ferrocenium sites are converted to ferrocene, the cation-blocking behavior is eliminated. Thus, the functionalized films behave as a membrane featuring bias-switchable permselectivity for anions (blocking behavior toward cations).

The combined findings have important implications for the use of MOF films as electrocatalysts, as electroanalytical devices, and as photoelectrodes in electrochemical cells. One could imagine, for example, using the cation exclusion behavior to advantage in photoelectrochemical applications by inhibiting back electron transfer from a dissolved cation to a light-harvesting site within the MOF, even when MOF channels are sufficiently large to admit the cations. Conversely, if the exclusion effect is overlooked, one could envision difficulty in accessing electrocatalysts within a MOF. Ion-exclusion effects can be suppressed, however, by raising the electrolyte concentration to a value similar to or greater than the concentration of fixed cationic (or anionic) sites within the MOF.

EXPERIMENTAL METHODS

NU-1000 was synthesized and activated using a published procedure[37] and then deposited in thin-film form on conductive glass (fluorine-doped tin oxide (FTO) coated glass) via electrophoresis of a suspension in toluene, as previously described;[4] see the Supporting Information for specifics. Also included in the Supporting Information are chemical sources and details of electrochemistry, PXRD, ^1H NMR, CW-ESR, and other experiments.

ASSOCIATED CONTENT

Supporting Information

Detailed NU-1000 synthesis procedure, chemical sources as well as details of electrochemistry, PXRD, ^1H NMR, CW-ESR, and other experiments. This material is available free of charge via the Internet at http://pubs.acs.org.

AUTHOR INFORMATION

Corresponding Authors

*E-mail: j-hupp@northwestern.edu (J.T.H.).
*E-mail: o-farha@northwestern.edu (O.K.F.).

Notes

The authors declare no competing financial interest.

DOI: 10.1021/acs.jpclett.5b00019
J. Phys. Chem. Lett. 2015, 6, 586−591

■ ACKNOWLEDGMENTS

This work was supported by the U.S. Department of Energy, Office of Science, Office of Basic Energy Sciences, Grant No. DE-FG02-87ER13808 (J.T.H.) and Grant No. DE-FG02-99ER14999 (M.R.W.), and by Northwestern University (O.K.F.). I.H. thanks the U.S−Israel Fulbright program for a postdoctoral fellowship.

■ REFERENCES

(1) Betard, A.; Fischer, R. A. Metal−Organic Framework Thin Films: From Fundamentals to Applications. *Chem. Rev.* **2012**, *112*, 1055−1083.

(2) Shekhah, O.; Wang, H.; Paradinas, M.; Ocal, C.; Schupbach, B.; Terfort, A.; Zacher, D.; Fischer, R. A.; Woll, C. Controlling Interpenetration in Metal−Organic Frameworks by Liquid-Phase Epitaxy. *Nat. Mater.* **2009**, *8*, 481−484.

(3) Hermes, S.; Schroder, F.; Chelmowski, R.; Woll, C.; Fischer, R. A. Selective Nucleation and Growth of Metal−Organic Open Framework Thin Films on Patterned COOH/CF_3-Terminated Self-Assembled Monolayers on Au(111). *J. Am. Chem. Soc.* **2005**, *127*, 13744−13745.

(4) Hod, I.; Bury, W.; Karlin, D. M.; Deria, P.; Kung, C.-W.; Katz, M. J.; So, M.; Klahr, B.; Jin, D.; Chung, Y.-W.; et al. Directed Growth of Electroactive Metal−Organic Framework Thin Films Using Electrophoretic Deposition. *Adv. Mater.* **2014**, *26*, 6295−6300.

(5) Li, M. Y.; Dinca, M. Reductive Electrosynthesis of Crystalline Metal−Organic Frameworks. *J. Am. Chem. Soc.* **2011**, *133*, 12926−12929.

(6) Bradshaw, D.; Garai, A.; Huo, J. Metal−Organic Framework Growth at Functional Interfaces: Thin Films and Composites for Diverse Applications. *Chem. Soc. Rev.* **2012**, *41*, 2344−2381.

(7) Tu, M.; Wannapaiboon, S.; Fischer, R. A. Liquid Phase Stepwise Growth of Surface Mounted Metal−Organic Frameworks for Exploratory Research and Development of Applications. *Inorg. Chem. Front.* **2014**, *1*, 442−463.

(8) Zacher, D.; Shekhah, O.; Woll, C.; Fischer, R. A. Thin Films of Metal−Organic Frameworks. *Chem. Soc. Rev.* **2009**, *38*, 1418−1429.

(9) Kung, C.-W.; Chang, T.-H.; Chou, L.-Y.; Hupp, J. T.; Farha, O.; Ho, K.-C. Post Metalation of Solvothermally Grown Electroactive Porphyrin Metal−Organic Framework Thin Films. *Chem. Commun.* **2014**, DOI: 10.1039/c4cc09272d.

(10) Ahrenholtz, S. R.; Epley, C. C.; Morris, A. J. Solvothermal Preparation of an Electrocatalytic Metalloporphyrin MOF Thin Film and Its Redox Hopping Charge-Transfer Mechanism. *J. Am. Chem. Soc.* **2014**, *136*, 2464−2472.

(11) Allendorf, M. D.; Schwartzberg, A.; Stavila, V.; Talin, A. A. A Roadmap to Implementing Metal−Organic Frameworks in Electronic Devices: Challenges and Critical Directions. *Chem.—Eur. J.* **2011**, *17*, 11372−11388.

(12) Lu, G.; Farha, O. K.; Zhang, W. N.; Huo, F. W.; Hupp, J. T. Engineering ZIF-8 Thin Films for Hybrid MOF-Based Devices. *Adv. Mater.* **2012**, *24*, 3970−3974.

(13) Brown, A. J.; Brunelli, N. A.; Eum, K.; Rashidi, F.; Johnson, J. R.; Koros, W. J.; Jones, C. W.; Nair, S. Interfacial Microfluidic Processing of Metal−Organic Framework Hollow Fiber Membranes. *Science* **2014**, *345*, 72−75.

(14) Fateeva, A.; Chater, P. A.; Ireland, C. P.; Tahir, A. A.; Khimyak, Y. Z.; Wiper, P. V.; Darwent, J. R.; Rosseinsky, M. J. A Water-Stable Porphyrin-Based Metal−Organic Framework Active for Visible-Light Photocatalysis. *Angew. Chem., Int. Ed.* **2012**, *51*, 7440−7444.

(15) Lin, W. B. Metal−Organic Frameworks for Solar Energy Utilization. *Abstr. Pap. Am. Chem. Soc.* **2012**, *244*, 393−394.

(16) Silva, C. G.; Luz, I.; Xamena, F. X. L. I.; Corma, A.; Garcia, H. Water Stable Zr-Benzenedicarboxylate Metal−Organic Frameworks as Photocatalysts for Hydrogen Generation. *Chem.—Eur. J.* **2010**, *16*, 11133−11138.

(17) Wang, J. L.; Wang, C.; Lin, W. B. Metal−Organic Frameworks for Light Harvesting and Photocatalysis. *ACS Catal.* **2012**, *2*, 2630−2640.

(18) Faunce, T.; Styring, S.; Wasielewski, M. R.; Brudvig, G. W.; Rutherford, A. W.; Messinger, J.; Lee, A. F.; Hill, C. L.; deGroot, H.; Fontecave, M.; et al. Artificial Photosynthesis as a Frontier Technology for Energy Sustainability. *Energy Environ. Sci.* **2013**, *6*, 1074−1076.

(19) Son, H. J.; Jin, S. Y.; Patwardhan, S.; Wezenberg, S. J.; Jeong, N. C.; So, M.; Wilmer, C. E.; Sarjeant, A. A.; Schatz, G. C.; Snurr, R. Q.; et al. Light-Harvesting and Ultrafast Energy Migration in Porphyrin-Based Metal−Organic Frameworks. *J. Am. Chem. Soc.* **2013**, *135*, 862−869.

(20) Lee, C. Y.; Farha, O. K.; Hong, B. J.; Sarjeant, A. A.; Nguyen, S. T.; Hupp, J. T. Light-Harvesting Metal−Organic Frameworks (MOFs): Efficient Strut-to-Strut Energy Transfer in Bodipy and Porphyrin-Based MOFs. *J. Am. Chem. Soc.* **2011**, *133*, 15858−15861.

(21) So, M. C.; Jin, S.; Son, H. J.; Wiederrecht, G. P.; Farha, O. K.; Hupp, J. T. Layer-by-Layer Fabrication of Oriented Porous Thin Films Based on Porphyrin-Containing Metal−Organic Frameworks. *J. Am. Chem. Soc.* **2013**, *135*, 15698−15701.

(22) Jin, S. Y.; Son, H. J.; Farha, O. K.; Wiederrecht, G. P.; Hupp, J. T. Energy Transfer from Quantum Dots to Metal−Organic Frameworks for Enhanced Light Harvesting. *J. Am. Chem. Soc.* **2013**, *135*, 955−958.

(23) Wade, C. R.; Li, M. Y.; Dinca, M. Facile Deposition of Multicolored Electrochromic Metal−Organic Framework Thin Films. *Angew. Chem., Int. Ed.* **2013**, *52*, 13377−13381.

(24) Kung, C. W.; Wang, T. C.; Mondloch, J. E.; Fairen-Jimenez, D.; Gardner, D. M.; Bury, W.; Klingsporn, J. M.; Barnes, J. C.; Van Duyne, R.; Stoddart, J. F.; et al. Metal−Organic Framework Thin Films Composed of Free-Standing Acicular Nanorods Exhibiting Reversible Electrochromism. *Chem. Mater.* **2013**, *25*, 5012−5017.

(25) Usov, P. M.; Fabian, C.; D'Alessandro, D. M. Rapid Determination of the Optical and Redox Properties of a Metal−Organic Framework via in situ Solid State Spectroelectrochemistry. *Chem. Commun.* **2012**, *48*, 3945−3947.

(26) Burgmayer, P.; Murray, R. W. Ion Gate Electrodes — Polypyrrole as a Switchable Ion Conductor Membrane. *J. Phys. Chem.* **1984**, *88*, 2515−2521.

(27) Burgmayer, P.; Murray, R. W. An Ion Gate Membrane — Electrochemical Control of Ion Permeability through a Membrane with an Embedded Electrode. *J. Am. Chem. Soc.* **1982**, *104*, 6139−6140.

(28) Naegeli, R.; Redepenning, J.; Anson, F. C. Influence of Supporting Electrolyte Concentration and Composition on Formal Potentials and Entropies of Redox Couples Incorporated in Nafion Coatings on Electrodes. *J. Phys. Chem.* **1986**, *90*, 6227−6232.

(29) Redepenning, J.; Anson, F. C. Permselectivities of Polyelectrolyte Electrode Coatings as Inferred from Measurements with Incorporated Redox Probes or Concentration Cells. *J. Phys. Chem.* **1987**, *91*, 4549−4553.

(30) Newton, M. R.; Bohaty, A. K.; White, H. S.; Zharov, I. Chemically Modified Opals as Thin Permselective Nanoporous Membranes. *J. Am. Chem. Soc.* **2005**, *127*, 7268−7269.

(31) Mondloch, J. E.; Katz, M. J.; Planas, N.; Semrouni, D.; Gagliardi, L.; Hupp, J. T.; Farha, O. K. Are Zr_6-Based MOFs Water Stable? Linker Hydrolysis vs. Capillary-Force-Driven Channel Collapse. *Chem. Commun.* **2014**, *50*, 8944−8946.

(32) DeCoste, J. B.; Peterson, G. W.; Jasuja, H.; Glover, T. G.; Huang, Y. G.; Walton, K. S. Stability and Degradation Mechanisms of Metal−Organic Frameworks Containing the $Zr_6O_4(OH)_4$ Secondary Building Unit. *J. Mater. Chem. A* **2013**, *1*, 5642−5650.

(33) deKrafft, K. E.; Boyle, W. S.; Burk, L. M.; Zhou, O. Z.; Lin, W. B. Zr- and Hf-Based Nanoscale Metal−Organic Frameworks as Contrast Agents for Computed Tomography. *J. Mater. Chem.* **2012**, *22*, 18139−18144.

(34) Vermoortele, F.; Ameloot, R.; Vimont, A.; Serre, C.; De Vos, D. An Amino-Modified Zr-Terephthalate Metal−Organic Framework as an Acid−Base Catalyst for Cross-Aldol Condensation. *Chem. Commun.* **2011**, *47*, 1521−1523.

DOI: 10.1021/acs.jpclett.5b00019
J. Phys. Chem. Lett. 2015, 6, 586−591

(35) Bon, V.; Senkovska, I.; Weiss, M. S.; Kaskel, S. Tailoring of Network Dimensionality and Porosity Adjustment in Zr- and Hf-Based MOFs. *CrystEngComm* **2013**, *15*, 9572−9577.
(36) Morris, W.; Volosskiy, B.; Demir, S.; Gandara, F.; McGrier, P. L.; Furukawa, H.; Cascio, D.; Stoddart, J. F.; Yaghi, O. M. Synthesis, Structure, and Metalation of Two New Highly Porous Zirconium Metal−Organic Frameworks. *Inorg. Chem.* **2012**, *51*, 6443−6445.
(37) Mondloch, J. E.; Bury, W.; Fairen-Jimenez, D.; Kwon, S.; DeMarco, E. J.; Weston, M. H.; Sarjeant, A. A.; Nguyen, S. T.; Stair, P. C.; Snurr, R. Q.; et al. Vapor-Phase Metalation by Atomic Layer Deposition in a Metal−Organic Framework. *J. Am. Chem. Soc.* **2013**, *135*, 10294−10297.
(38) Deria, P.; Bury, W.; Hupp, J. T.; Farha, O. K. Versatile Functionalization of the NU-1000 Platform by Solvent-Assisted Ligand Incorporation. *Chem. Commun.* **2014**, *50*, 1965−1968.
(39) Deria, P.; Mondloch, J. E.; Tylianakis, E.; Ghosh, P.; Bury, W.; Snurr, R. Q.; Hupp, J. T.; Farha, O. K. Perfluoroalkane Functionalization of NU-1000 via Solvent-Assisted Ligand Incorporation: Synthesis and CO_2 Adsorption Studies. *J. Am. Chem. Soc.* **2013**, *135*, 16801−16804.
(40) Planas, N.; Mondloch, J. E.; Tussupbayev, S.; Borycz, J.; Gagliardi, L.; Hupp, J. T.; Farha, O. K.; Cramer, C. J. Defining the Proton Topology of the Zr-6-Based Metal−Organic Framework NU-1000. *J. Phys. Chem. Lett.* **2014**, *5*, 3716−3723.
(41) Hwang, Y.; Sohn, H.; Phan, A.; Yaghi, O. M.; Candler, R. N. Dielectrophoresis-Assembled Zeolitic Imidazolate Framework Nanoparticle-Coupled Resonators for Highly Sensitive and Selective Gas Detection. *Nano Lett.* **2013**, *13*, 5271−5276.
(42) Mao, Y.; Thomas, J. K. Photochemical-Reactions of Pyrene on Surfaces of γ-Alumina and Silica−Alumina. *Langmuir* **1992**, *8*, 2501−2508.
(43) Mao, Y.; Thomas, J. K. Chemical-Reactions of Molecular-Oxygen in Surface-Mediated Photolysis of Aromatic-Compounds on Silica-Based Surfaces. *J. Phys. Chem.* **1995**, *99*, 2048−2056.
(44) Wilkinson, A. D. M. a. A. *IUPAC Compendium of Chemical Terminology*, 2nd ed. (the "Gold Book"); Blackwell Scientific Publications: Oxford, U.K., 1997.
(45) Spiegler, K. S.; Yoest, R. L.; Wyllie, M. R. J. Electrical Potentials Across Porous Plugs and Membranes — Ion-Exchange Resin-Solution Systems. *Discuss. Faraday. Soc.* **1956**, 174−185.
(46) It is important to note that although the films are not fully covered with MOF particles and possess exposed FTO sites, at low enough ionic strengths, the permselectivity is retained. This effect has been explored before in several types of polyionic permselective films.[23,24,37]
(47) Sutin, N.; Brunschwig, B. S.; Creutz, C.; Winkler, J. R. Nuclear Reorganization Barriers to Electron-Transfer. *Pure Appl. Chem.* **1988**, *60*, 1817−1830.

DOI: 10.1021/acs.jpclett.5b00019
J. Phys. Chem. Lett. 2015, 6, 586−591